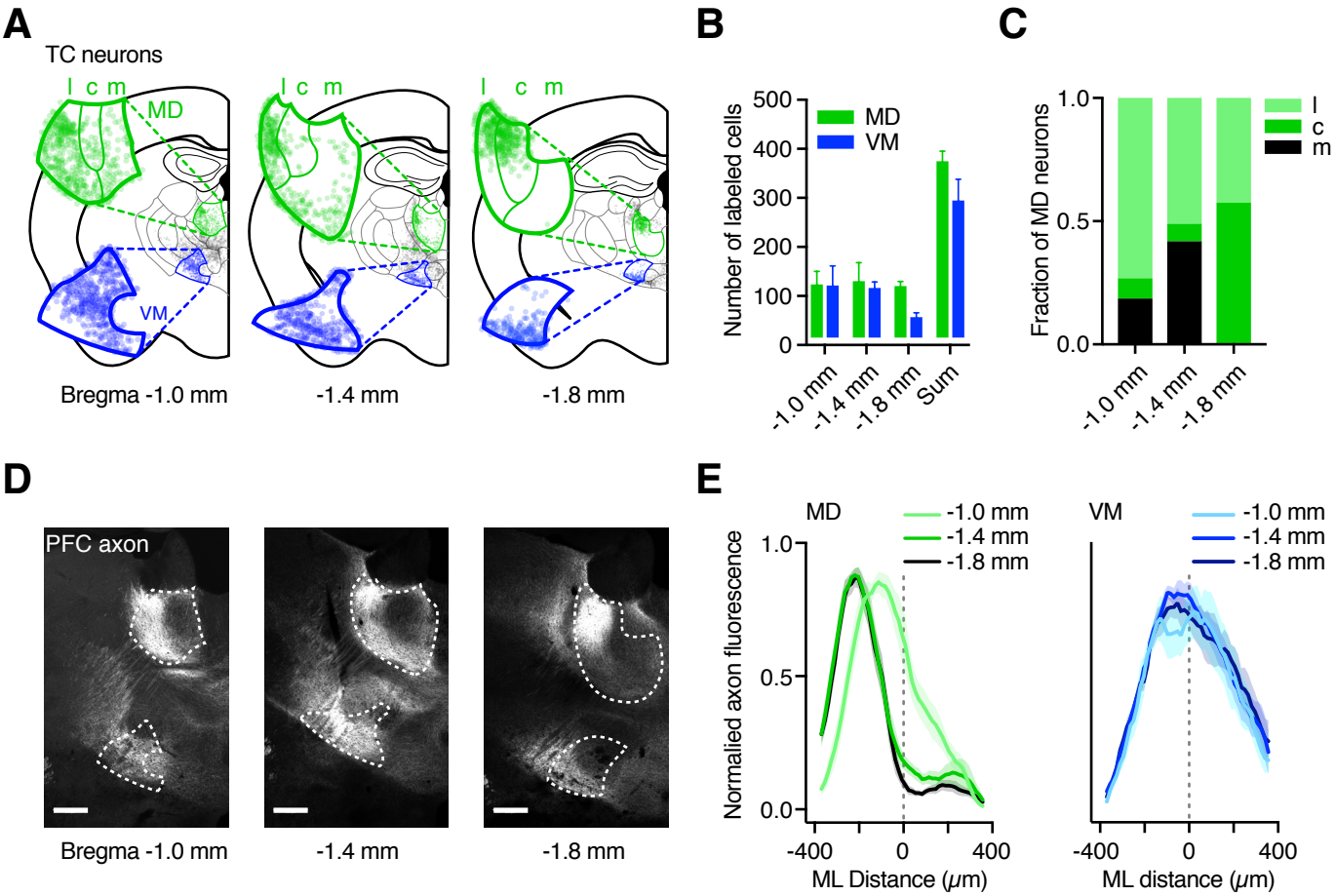

Collins, Anastasiades et al., Figure S1

Figure S1. Anatomical definition of thalamic regions that interact with PFC.

Related to Figure 1.

(A) Distribution of retrogradely labeled thalamo-cortical (TC) neurons following CTB injection into the prelimbic subdivision of the medial prefrontal cortex (PFC). Mediodorsal (MD) (green) and ventromedial (VM) (blue) thalamic nuclei are shown at three rostro-caudal (RC) coordinates (from left to right) -1.0 mm, -1.4 mm & -1.8 mm (all relative to Bregma). The distribution of retrogradely labeled TC neurons is highlighted in the enlarged diagrams with MD (green) and VM (blue) neurons shown as individual points. MD is divided into 3 subregions, where l = lateral, c = central and m = medial. Retrogradely labeled TC neurons that fall outside MD and VM are shown in grey. n = 6 mice.

(B) Summary of the number of retrogradely labeled TC neurons in MD (green) and VM (blue) at the three RC coordinates shown in (A) and summed across all three areas. A similar number of MD and VM neurons target PL PFC.

(C) Summary showing the number of retrogradely labeled TC neurons in different subregions of MD at the RC coordinates shown in (A). Prelimbic-projecting neurons are primarily localized in lateral aspects of MD, but this relationship shifts across the RC axis.

(D) Confocal images showing distribution of anterogradely labeled cortico-thalamic (CT) axons following injection of AAV-DIO-ChR2-YFP into prelimbic PFC of Emx1-Cre mice. Axon distributions are shown at the three RC coordinates shown in (A). MD and VM are demarcated by white outlines. PFC axons target both MD and VM across a range of RC coordinates. Scale bars: 300 µm.

(E) Summary quantifying the distribution of PFC axon in MD (left) and VM (right) at the three RC coordinates shown in (A). PFC axons are biased towards lateral MD, as observed for PFC projecting TC neurons. n = 6 mice.

Values are mean ± SEM.

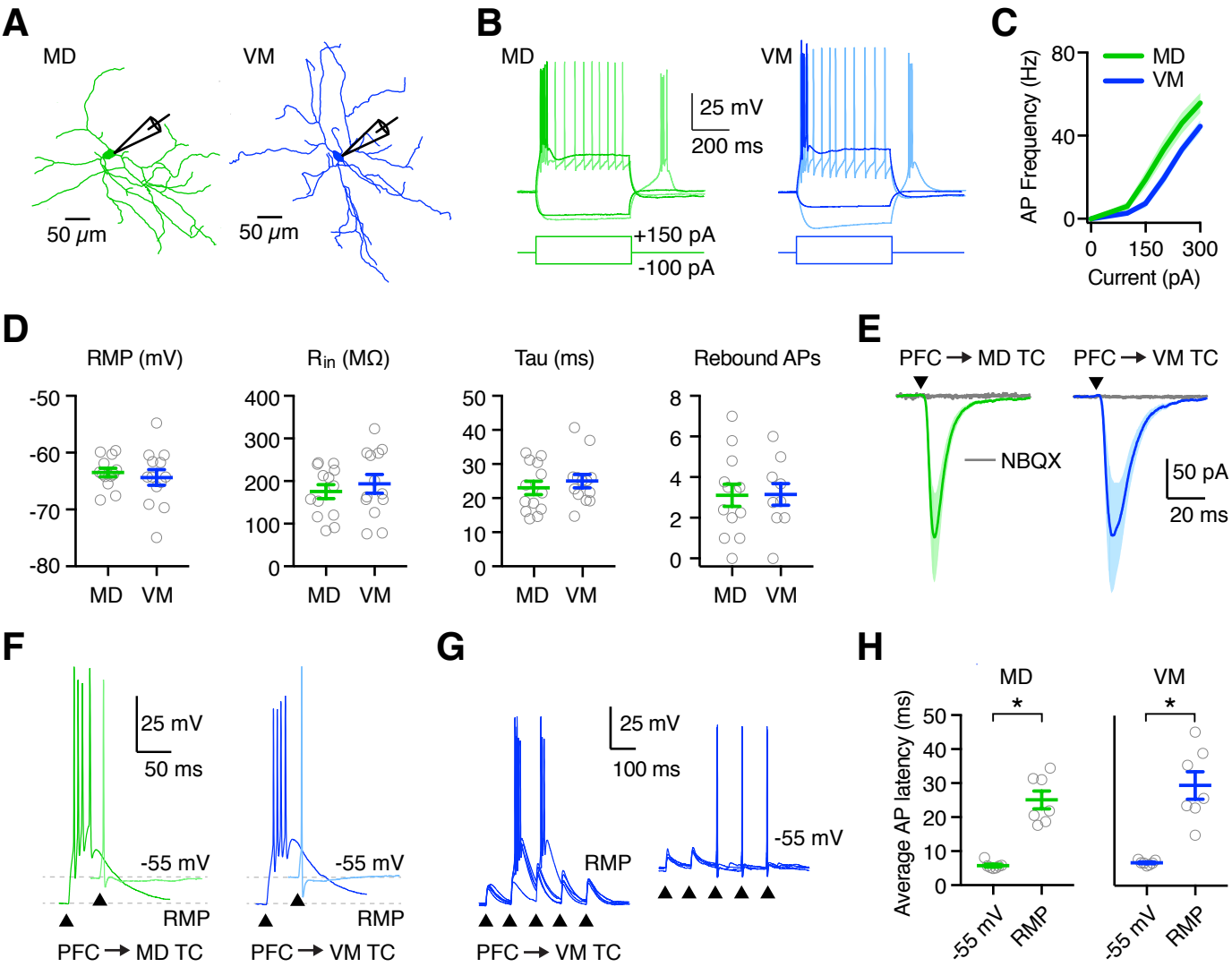

Collins, Anastasiades et al., Figure S2

Figure S2. Intrinsic properties and synaptic responses of TC neurons.

Related to Figure 1.

(A) Example reconstructions of PFC-projecting TC neurons in MD (left, green) and VM (right, blue).

(B) Current-clamp responses to +150 and -100 pA current steps recorded from PFC-projecting TC neurons in MD (left, green) and VM (right, blue), held at -55 mV (light traces) and resting membrane potential (RMP, dark traces) (-65 mV for both cells). Traces are baseline subtracted for display purposes. Examples at each potential are from the same cell.

(C) Summary of action potential (AP) firing frequency evoked by current steps of increasing size in MD and VM TC neurons at RMP. n = 13 cells each, 10 mice.

(D) From left to right, RMP, input resistance (R_{in}), membrane time constant (Tau), and number of rebound APs for MD (green) and VM (blue) TC neurons. All values were calculated from responses measured at RMP except rebound APs, which could only be elicited at -55 mV. n = 13 cells each, 10 mice.

(E) PFC-evoked AMPA-R EPSCs at TC neurons in (left, green) and VM (right, blue), recorded at -60 mV in response to 4 ms LED pulse (triangle). Solid lines are average and shaded regions are SEM. Gray trace shows average response after NBQX wash-in.

(F) PFC-evoked firing of PFC-projecting TC neurons in MD (left) and VM (right), recorded at RMP (-64 mV for both cells) and -55 mV in response to 4 ms LED pulse (triangle).

(G) PFC-evoked EPSPs and APs of VM TC neurons, recorded at RMP (left) and -55 mV (right) in response to 10 Hz PFC stimulation trains (triangles). Each panel shows five example traces from the same cell. Data in G-H are from experiments in Fig. 1D-E.

(H) Summary of AP latency in MD (left) and VM (right) neurons for the first light pulse to evoke AP firing. APs occur at short latency at -55 mV but are delayed at RMP.

Values are mean ± SEM. * = $p < 0.05$.

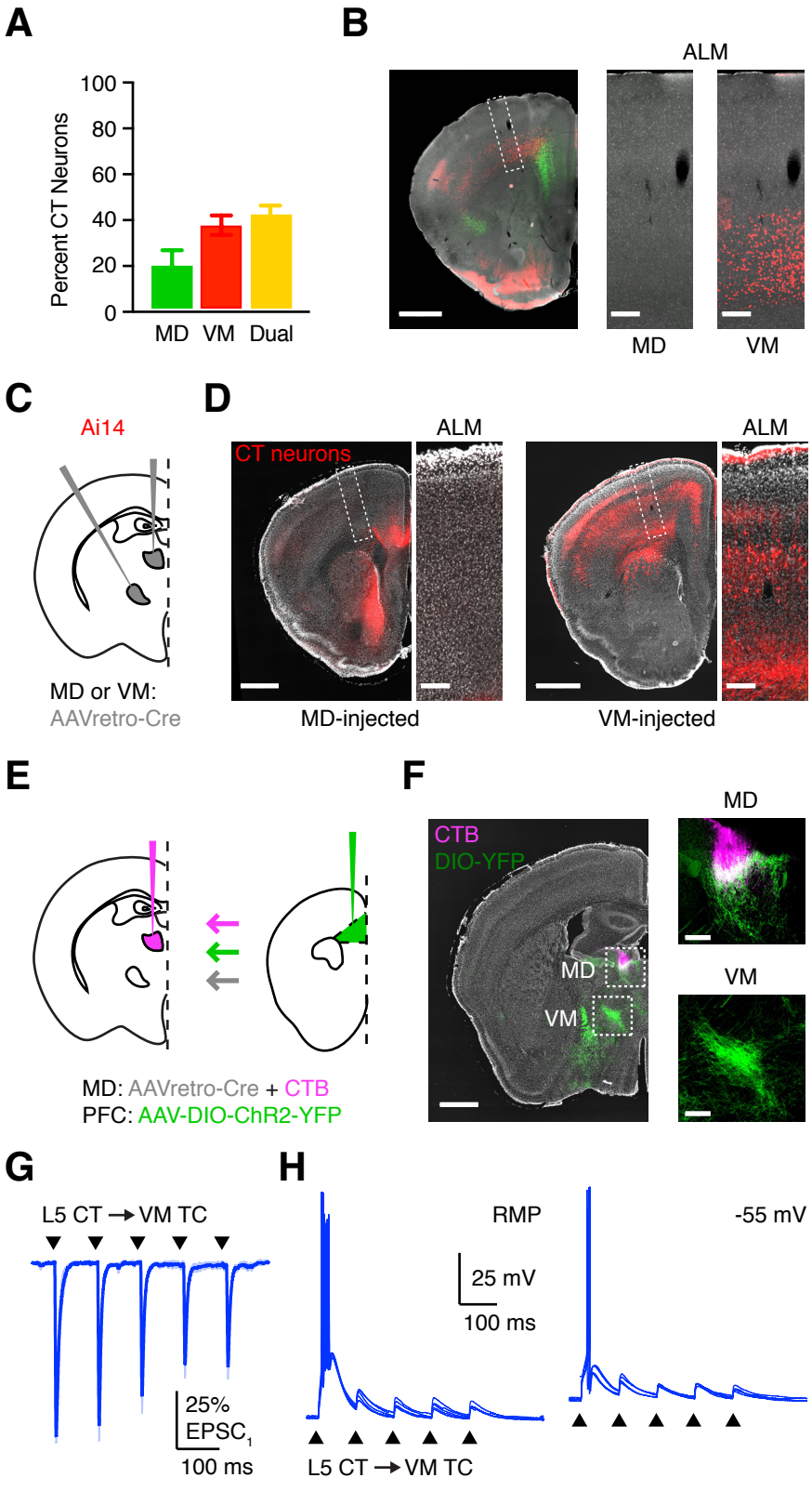

Collins, Anastasiades et al., Figure S3

Figure S3. Anatomical characterization of CT neurons that project to MD and VM.

Related to Figures 2 & 3.

(A) Summary quantifying the distribution of MD-projecting (green), VM-projecting (red), and dual-labeled (yellow) CT neurons as a fraction of all CT neurons in prelimbic PFC. Data in A-B are from experiments in Fig. 2A-B.

(B) Left: Representative image of retrogradely labeled CT neurons, following CTB injection into MD (green) and VM (red) of wild-type mice. Dashed box highlights region of anterior lateral motor cortex (ALM) from which enlarged images are shown. Middle: Enlarged image of ALM, showing absence of retrogradely labeled cells projecting to MD. Right: Enlarged image of ALM, showing presence of retrogradely labeled VM-projecting CT cells in L5 and 6. Grayscale images show DAPI labeling. Scale bars: 1000 μm (left) & 200 μm (middle, right).

(C) Injection scheme for detecting retrogradely labeled CT neurons. AAVretro-Cre was injected into either MD or VM of Ai14 reporter mice, followed by imaging in frontal cortices. These same mice were also injected with CTB in the thalamic injection site and AAVs expressing Cre-dependent YFP in prelimbic PFC as in E-F, not shown here for clarity. n = 3 mice each.

(D) Left: Representative image of retrogradely labeled CT neurons following AAVretro-Cre injection into MD. Enlarged image shows absence of tdTomato+ neurons in ALM. Right: Same, following injection in VM. Enlarged image shows labelling in motor regions, including ALM. Scale bars: 1000 μm & 200 μm, respectively.

(E) Schematic of injection scheme for detecting diverging projections of CT neurons, showing injection of AAVretro-Cre and CTB in MD, along with AAVs expressing Cre-dependent YFP in prelimbic PFC. These experiments were performed in Ai14 mice to further confirm injection site based on the presence (for VM) or absence (for MD) of labeling in motor cortex, shown in C-D.

(F) Left: Representative image showing injection site in MD and retrogradely labeled cross-thalamic CT axons in both MD and VM. Grayscale images represent DAPI labeling. Dashed boxes are magnified in smaller images at right. Scale bars: 1000 μm (larger image) or 200 μm.

(G) L5 CT-evoked EPSCs in VM TC neurons at -60 mV, recorded in response to 10 Hz LED stimulation trains (triangles). Data are from experiments in Fig. 3C.

(H) L5 CT-evoked EPSPs and action potentials (APs) in VM TC neurons at RMP (left) and -55 mV (right), recorded in response to 10 Hz LED stimulation trains (triangles). Each example shows four traces from the same cell. Data are from experiments in Fig. 3D-E.

Values are mean ± SEM.

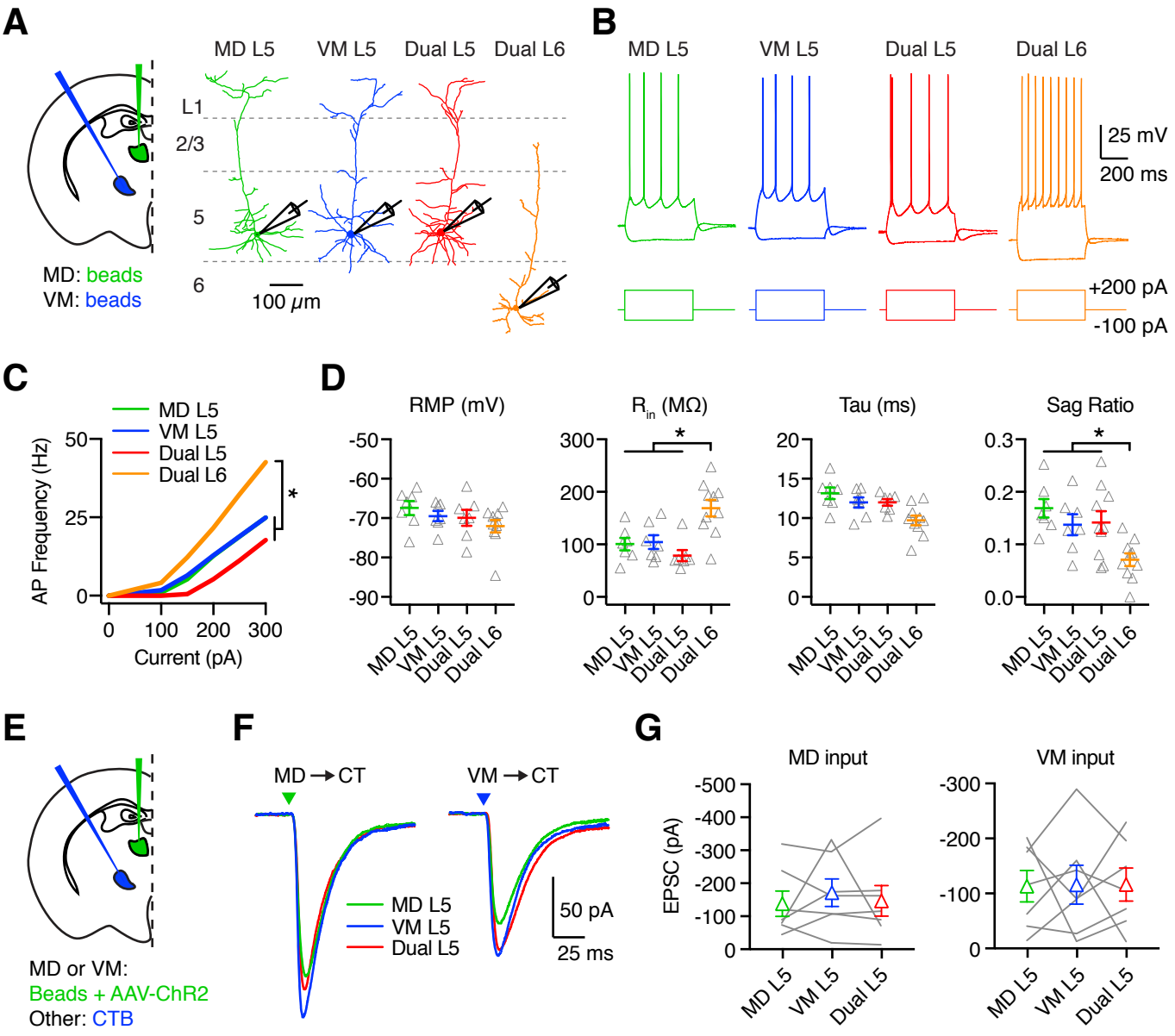

Collins, Anastasiades et al., Figure S4

Figure S4. Intrinsic properties and synaptic responses of L5 and L6 CT neurons.

Related to Figure 4.

(A) Injection schematic and neuronal morphologies for retrogradely labeled MD-, VM-, or dual-projecting CT neurons in PFC.

(B) Current-clamp responses to +200 and -100 pA current steps from CT neurons recorded at RMP (MD: -66 mV; VM: -66 mV, Dual L5: -67 mV, Dual L6: -72 mV).

(C) Summary of action potential (AP) firing frequency evoked by current steps of increasing size in CT neurons at RMP. n = 7 cells MD L5, 7 cells VM L5, 5 mice; 7 cells Dual L5, 5 mice; 10 cells Dual L6, 6 mice.

(D) From left to right: Resting membrane potential (RMP), input resistance (R_{in}), membrane time constant (Tau), and Sag Ratio (mediated by h-current) for CT neurons. Open triangles show data from individual cells. n = 7 cells MD L5, 7 cells VM L5, 5 mice; 7 cells Dual L5, 5 mice; 10 cells Dual L6, 6 mice.

(E) Injection schematic for recording thalamus-evoked EPSCs in MD-, VM-, and dual-projecting L5 CT neurons. Retrobeads and AAV-ChR2 were injected in MD or VM, while CTB was injected in the other nucleus.

(F) Average MD- (left), or VM-evoked (right) EPSCs recorded from triplets of MD-only, VM-only and dual-projecting L5 CT neurons. MD input: n = 7 triplets, 4 mice; VM input: n = 7 triplets, 4 mice.

(G) Summary of EPSC amplitudes for MD (left) or VM (right) input to MD-only, VM-only and dual-projecting L5 CT neurons.

Values are mean ± SEM. * = $p < 0.05$

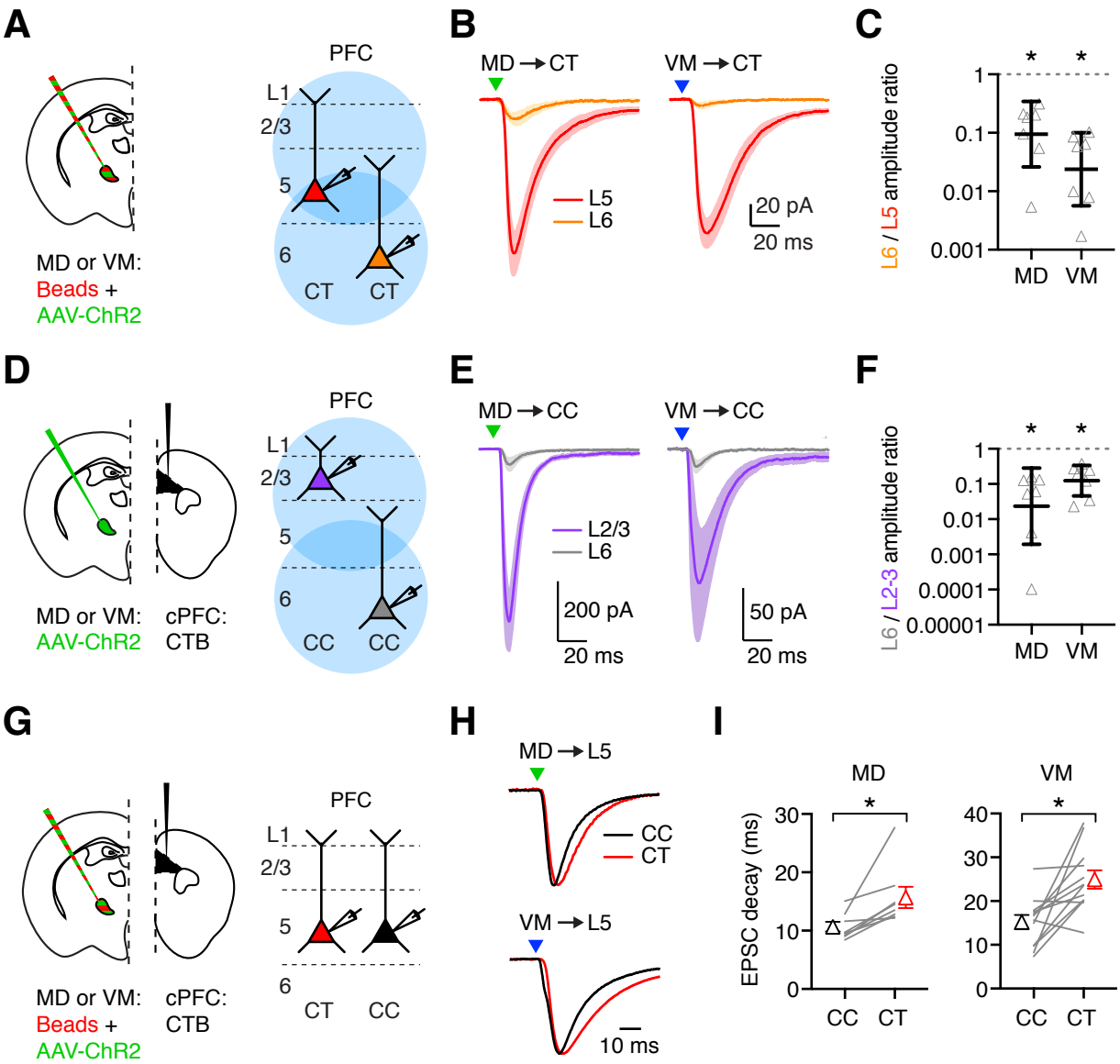

Collins, Anastasiades et al., Figure S5

Figure S5. Properties of thalamic EPSCs at CT and CC neurons.

Related to Figures 4, 5 & 6.

(A) Injection schematic and recording scheme. Recordings were made from retrogradely labeled L5 and L6 CT neurons in PFC after injection of both retrobeads and AAV-ChR2 into either MD or VM. Thalamic inputs were stimulated at both 350 μm from the midline for L5 CT neurons (upper blue circle), and directly over the soma of L6 CT neurons (lower blue circle).

(B) EPSCs in L5 and L6 CT neurons evoked by MD (left) or VM (right) input, with both inputs evoking negligible response onto L6 CT neurons, confirming that the absence of EPSCs was not due to failure to stimulate thalamic synapses in deeper layers. MD input: n = 7 pairs, 3 mice; VM input: n = 7 pairs, 3 mice.

(C) Summary of L6 / L5 EPSC amplitude ratio from (B), stimulating at 350 μm from the midline for L5 CT neurons, and over the soma of L6 CT neurons. Note logarithmic axis.

(D-F) Similar to (A-C) for L2/3 and L6 CC neurons, again confirming that the absence of EPSCs was not due to failure to stimulate thalamic synapses in deeper layers. MD input: n = 7 pairs, 4 mice; VM input: 7 pairs, 3 mice.

(G) Injection schematic and recording scheme. Recordings were made from retrogradely labeled L5 CC and CT neurons in PFC after injection of CTB in cPFC and retrobeads and AAV-ChR2 in either MD or VM. Data in G-I are from experiments in Fig. 5A-D.

(H) Average EPSCs evoked by MD (top) and VM (bottom) inputs at pairs of L5 CC and CT neurons. CT responses have been peak scaled to the CC EPSC.

(I) Summary of EPSC decay for MD (left) and VM (right) inputs.

Values are geometric mean ± 95% CI (C,F) or mean ± SEM (I). * = $p < 0.05$

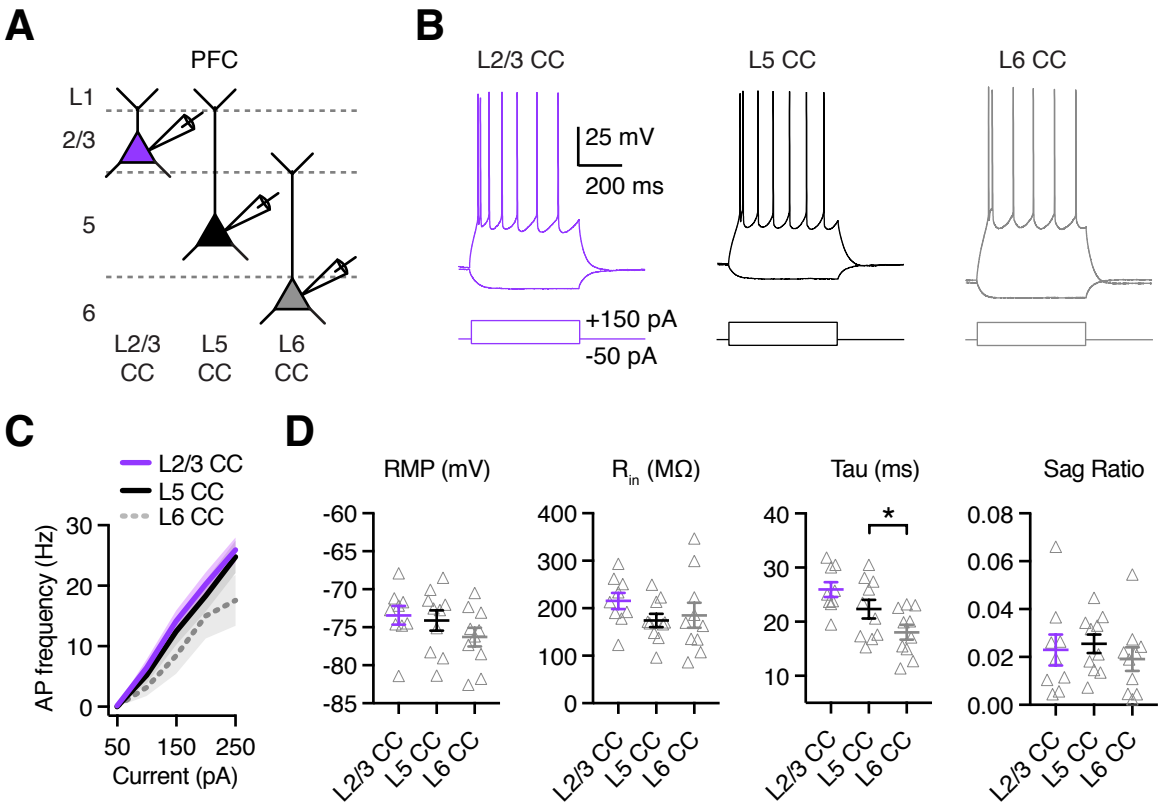

Collins, Anastasiades et al., Figure S6

Figure S6. Properties of CC neurons across layers.

Related to Figure 6.

(A) Recording scheme. Current-clamp recordings were made from retrogradely labeled CC neurons in L2/3, L5, and L6 of PFC.

(B) Current-clamp responses to +150 pA and -50 pA current steps for L2/3, L5 and L6 CC neurons at RMP.

(C) Summary of action potential (AP) firing frequency evoked by current steps of increasing size in L2/3, L5, and L6 CC neurons at RMP. n = 9 L2/3 CC cells, 10 L5 CC cells, 10 L6 CC cells, 14 mice.

(D) From left to right: RMP, input resistance (R_{in}), membrane time constant (Tau), and Sag Ratio (mediated by h-current) for L2/3, L5, and L6 CC neurons. Open triangles show data from individual cells. n = 9 L2/3 CC cells, 10 L5 CC cells, 10 L6 CC cells, 14 mice.

Values are mean ± SEM. * = $p < 0.05$

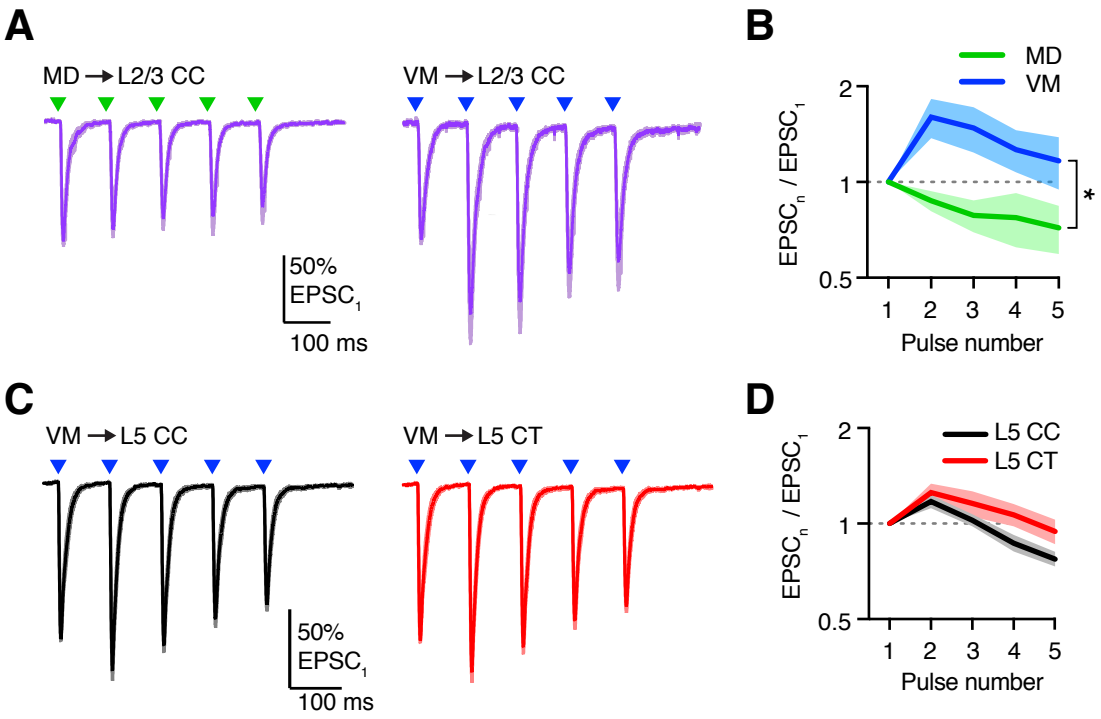

Collins, Anastasiades et al., Figure S7

Figure S7. Short-term dynamics of VM input to CC and CT neurons.

Related to Figure 7.

(A) Thalamus-evoked EPSCs from L2/3 CC neurons at -70 mV, in response to 10 Hz LED stimulation trains (triangles) of MD (left) or VM (right) inputs in the absence of inhibition, with EPSCs normalized to the first EPSC amplitude before averaging. MD input: n = 9 cells, 3 mice; VM input: n = 11 cells, 4 mice.

(B) Summary of paired-pulse ratio (PPR) for MD (green) and VM (inputs) for each pulse (n) in the train.

(C) EPSCs evoked by 10 Hz LED stimulation of VM inputs (blue triangles) inputs in L5 CC (left) and CT (right) neurons at -70 mV in the absence of inhibition. Each trace is normalized to the amplitude of the first EPSC before averaging. Similar experiments were not possible for MD in the absence of inhibition due to the strong input to L2/3. L5 CC: n = 8 cells, 3 mice; L5 CT: n = 6 cells, 3 mice.

(D) Summary of paired-pulse ratio (PPR) for L5 CC and CT neurons for data shown in (C). Values are mean ± SEM. * = $p < 0.05$

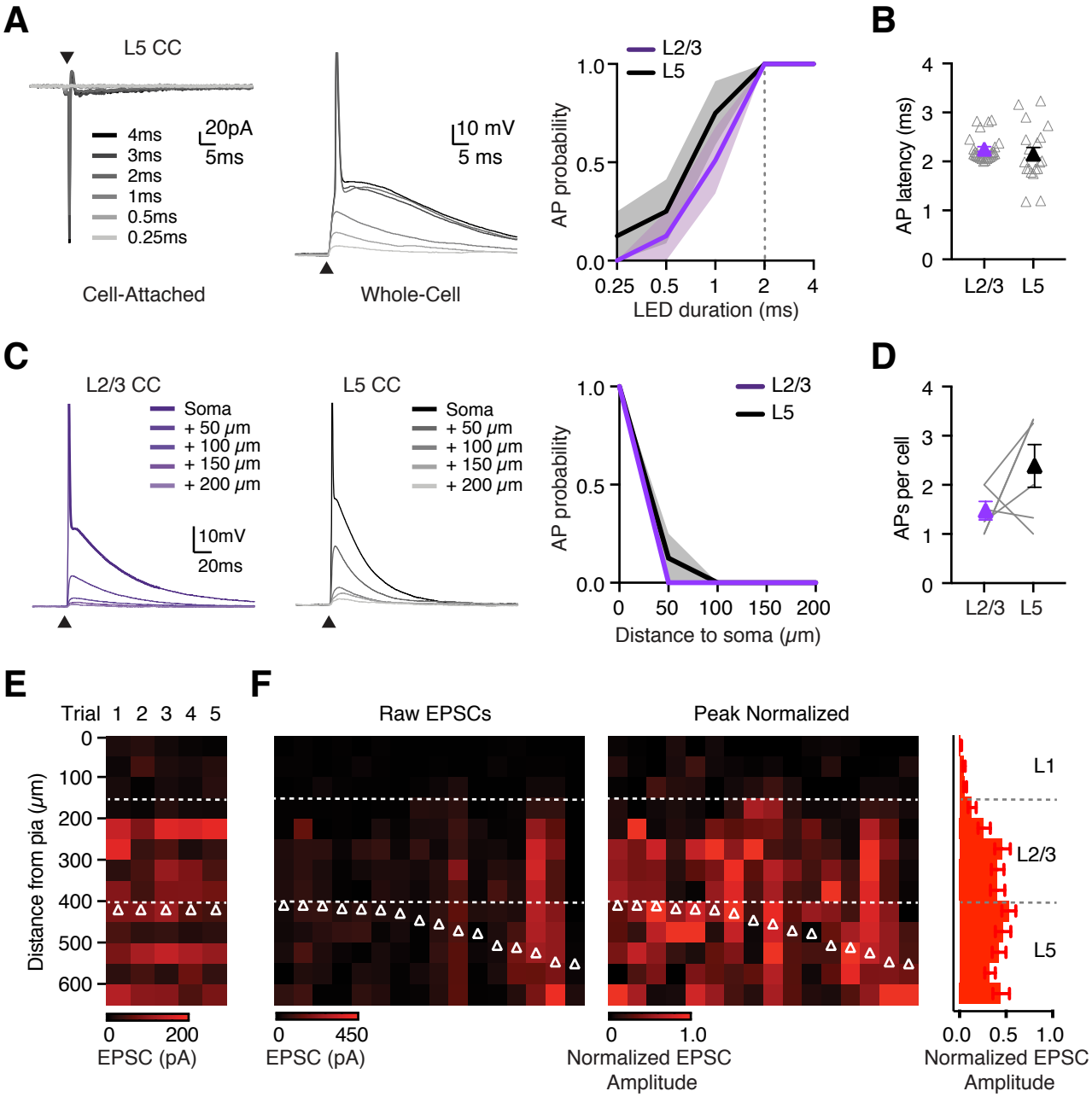

Collins, Anastasiades et al., Figure S8

Figure S8. Using soma-tagged optogenetics to study CC to CT connectivity.

Related to Figure 8.

(A) Left: Light-evoked action potentials (APs) from a st-ChroME-expressing L5 CC neuron during optogenetic stimulation (triangle) of increasing pulse duration. Recording was made in cell-attached configuration to avoid perturbing the intracellular environment. Middle: Similar firing was observed in whole-cell recordings of the same L5 CC neuron at RMP. Y–axis truncated to better highlight subthreshold responses. Right: Summary of AP probability across different pulse durations. Firing was similar for st-ChroME-expressing L2/3 and L5 CC neurons recorded pairwise from the same slice, using identical stimulus parameters within pairs. Dashed line indicates 2 ms pulse duration, at which firing was always observed in both L2/3 and L5 CC neurons. Data in A-D are from experiments in Fig. 8D-F.

(B) Summary of AP latency in response to 2 ms LED stimulation for st-ChroME-expressing L2/3 and L5 CC neurons. AP latency is rapid and similar in both populations. Open triangles show data from individual trials across multiple cells.

(C) Subthreshold and suprathreshold responses from st-ChroME-expressing L2/3 (left) and L5 (middle) CC neurons in response to optogenetic stimulation at increasing lateral distances from the soma. Y–axis truncated to better highlight subthreshold responses. Right: Summary of AP probability as a function of distance from the soma in the x-axis. Firing is restricted to stimulation at the soma for both L2/3 and L5 CC neurons.

(D) Summary of the total number of APs evoked per cell in response to cross-laminar stimulation for st-ChroME-expressing L2/3 and L5 neurons. In general, L5 cells were slightly more excitable than those in L2/3.

(E) CC-evoked EPSCs from a L5 CT neuron, evoked by local stimulation at varying distances from the pial surface. Each column represents a single trial. The soma location

of the recorded cell is indicated by a triangle. CC-evoked EPSCs are reliable and stable across trials.

(F) Left: Amplitudes of “raw” CC-evoked EPSCs in L5 CT neurons, evoked by local stimulation at varying distances from the pial surface. Each column represents a recorded neuron, with soma location indicated by triangle. Middle: Similar, but for amplitudes of peak-normalized EPSCs, in order to account for variability across individual neurons. Right: Summary of peak-normalized EPSC amplitude during stimulation at varying distances from the pial surface. Data in F are from experiments in Fig. 8G-I.

Values are mean ± SEM.